Supplemental Material (Online Only)

Absolute Geomagnetic Intensity Determinations on Formative Potsherds (1400–700 BC) from the Oaxaca Valley, Southwestern Mexico

M. Pétronille, A. Goguitchaichvili, J. Morales, C. Carvallo and Y. Hueda-Tanabe

Phase/ Age	Site	Potsherd/ Type[1]	Clay body and engobe	Estimated temperature of burning	Interior, exterior and border of potsherd
Tierras Largas (1400–1150 BC)	San José Mogote	OAX13 (A.R.B.)	Clay body contains 50% of clay minerals and 50% of non-plastic particles with a diameter of 1 to 4 mm (quartz, feldspar, iron micas, hornblende and augite). The red color of the engobe is due to iron oxides.	Around 700°C in oxidizing atmosphere, probably heated in open-air.	
		OAX16 (M.O.)	Minerals of the clay body[2] are identical to OAX13 but the orangy engobe has a high iron content and the clay is naturally orangy.	Around 700°C in oxidizing atmosphere.	
		OAX17 (T.L.B.P.)	Clay body[2] contains quartz, feldspar, iron micas, hornblende and augite. Brown color.	Similar to OAX13.	
	Tierras Largas	OAX05 (M.R.)	Minerals of the clay body[2] are similar to OAX16 but the engobe of "colored mud" has a high iron content and the clay is naturally reddish.	Around 700–720°C in oxidizing atmosphere.	
San José (1150–850 BC)	San José Mogote	OAX01 (A.Y.W.)	Clay body contains quartz, mica, feldspar, hornblende and sometimes garnet. Interior and exterior are light colored.	Around 720–760°C in oxidizing atmosphere.	
		OAX02 (D.W.)	Clay body contains feldspar, pyroxenes with quartz, or quartz and feldspar, in very thin kaolinite. The engobe is white kaolinite without iron and the clay is orangy.	Around 750–770°C varying from complete oxidation to small reduction.	
		OAX03 (C.F.R.B.)	Interior with white engobe, white and black for exterior.	No information.	
		OAX08 (S.J.R.W.)	Clay body contains hematite in red parts of the engobe.	No information.	
		OAX10 (L.H.P.)	Interior and exterior are brown.	Similar to OAX05.	
		OAX12 (F.C.)	Clay body[2] contains 30–35% of non-plastic particles with diameter of 0.1 to 1mm (quartz, biotite, feldspar and hornblende partially decomposed, sometimes garnet) in a base of kaolinite. The red engobe has a high content in iron and the clay is naturally orangy.	Identical to OAX05.	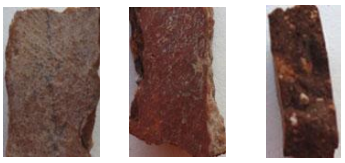
		OAX14 (S.J.B.W.)	Identical to OAX01. Interior and exterior are black/gray.	Around 700–720°C in strong reduction but small oxidation.	
		OAX15 (D.F.G.)	Fine texture of the clay body that contains quartz, amphiboles, pyroxenes and feldspar. Interior and exterior are gray.	Around 750°C in reducing atmosphere.	
	Barrio del Rosario Huitzo	OAX09 (L.G.)	Minerals of the clay body[2] are identical to OAX12 but there are volcanic particles of ignimbrite. Interior and exterior are gray.	Around 700–720°C in reducing atmosphere.	
	Origin ?	OAX11 (F.C.)	Identical to OAX12.	Similar to OAX05.	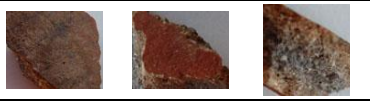
Guadalupe (850–700 BC)	San José Mogote	OAX06 (G.B.B.)	Interior and exterior are brown. The black mark on the exterior part is due to heating.	No information.	

[1] Classification of potsherds according to their type (see González Licón and Fernández Dávila (2005) for detailed explanations) : A.R.B.= Avelina Red-on-Buff; M.O.= Matadamas Orange; T.L.B.P.= Tierras Largas Burnished Plain; M.R.= Matadamas Red; A.Y.W.= Atoyac Yellow-White; D.W.= Delia White; C.F.R.B.= Clementina Fine Red-on-Buff; S.J.R.W.= San José Red-on-White; L.H.P.= Lupita Heavy Plain; F.C.= Fidencio Coarse; S.J.B.W.= San José Back-and-White; D.F.G.= Delfina Fine Gray; L.G.= Leandro Gray; G.B.B.= Guadalupe Burnished Brown.

[2] Potsherd for which clay body minerals come from Precambrian gneiss. No sure information is given for the other potsherds.

Supplemental material 1: Detailed list of the 15 studied potsherds from the Oaxaca Valley. From left to right (synthetized from González Licón and Fernández Dávila, 2005): phase in the Formative period (or Preclassic era) and associated ages; site of origin (their geographic coordinates are indicated in the main text); name of the potsherd and type (see note 1 above for more explanations); description of the clay body and of the engobe; estimation of firing temperature and associated atmosphere; photos of interior, exterior and border of potsherd.

Supplemental Material (Online Only)

Absolute Geomagnetic Intensity Determinations on Formative Potsherds (1400–700 BC) from the Oaxaca Valley, Southwestern Mexico

M. Pétronille, A. Goguitchaichvili, J. Morales, C. Carvallo and Y. Hueda-Tanabe

Potsherd/ Site	Phase/ Age	Specimen	N	ΔT (°C)	f	g	q	$F \pm \sigma F$ (μT)	F_{cor} (μT)	VADM (10^{22}Am^2)	Type
OAX01 (S.J.M.)	San José (1150–850 BC)	99O001A	7	350-540	0.28	0.82	4.36	18.4 ± 1.0	17.8	5.2	B
		99O001B	5	400-520	0.27	0.73	9.53	20.3 ± 0.4	19.6	5.7	B
		99O001C	7	350-540	0.39	0.83	6.77	19.7 ± 0.9	19.0	5.5	B
		99O001D	7	350-540	0.31	0.83	3.86	19.4 ± 1.3	19.2	5.6	B
		99O001E	10	200-540	0.51	0.88	11.48	19.5 ± 0.8	18.7	5.4	B
		99O001F	10	150-520	0.48	0.87	8.39	18.5 ± 0.9	17.6	5.1	B
Mean[1]								19.3	**18.6**	**5.4**	
σ[1]								0.7	**0.8**	**0.2**	
OAX02 (S.J.M.)	San José (1150–850 BC)	99O002A	Broken at 350°C.								
		99O002B	8	200-500	0.61	0.85	11.95	36.8 ± 1.6	32.8	9.5	A
		99O002C	Broken at 350°C.								
		99O002D	8	200-500	0.74	0.84	13.50	30.7 ± 1.4	28.1	8.2	A
		99O002E	5	250-450	0.54	0.74	10.71	23.7 ± 0.9	22.6	6.6	A
		99O002F	5	250-450	0.56	0.74	11.00	23.0 ± 0.9	22.0	6.4	A
Mean[1]								30.3	**27.8**	**8.0**	
σ[1]								6.7	**5.3**	**1.5**	
OAX03 (S.J.M.)	San José (1150–850 BC)	99O003A	Arai diagrams show a concave-up shape with two different slopes whereas Zijderveld projections show one component pointing to the origin.								C
		99O003B									C
		99O003C									C
		99O003D									C
		99O003E									C
		99O003F									C
OAX05 (T.L.)	Tierras Largas (1400–1150 BC)	99O005A	9	300-560	0.68	0.87	20.81	61.5 ± 1.8	58.4	16.9	A
		99O005D	Broken at 350°C.								
		99O005E	10	300-580	0.74	0.88	28.17	32.7 ± 0.8	30.1	8.7	A

		99O005F	10	300-580	0.75	0.87	31.67	36.3 ± 0.8	35.2	10.2	A
OAX06 (S.J.M.)	Guadalupe (850–700 BC)	99O006A	Broken at 400°C.								
		99O006B	12	200-580	0.88	0.90	42.69	36.2 ± 0.7	35.3	10.2	A
		99O006C	Zijderveld diagrams show many components.								
		99O006D	11	250-580	0.81	0.89	27.81	35.4 ± 0.9	34.2	9.9	A
		99O006E	12	200-580	0.79	0.90	20.83	31.1 ± 1.1	30.0	8.7	A
		99O006F	13	300-580	0.65	0.88	12.90	30.3 ± 1.4	28.9	8.4	A
Mean[1]								34.1	**33.0**	**9.6**	
***σ*[1]**								3.0	**3.1**	**0.9**	
OAX08 (S.J.M.)	San José (1150–850 BC)	99O008A	9	350-580	0.59	0.87	9.28	24.6 ± 1.4	23.3	6.8	A
		99O008B	7	350-540	0.43	0.82	9.55	27.3 ± 1.0	25.6	7.4	A
		99O008C	7	350-540	0.41	0.82	11.02	25.2 ± 0.8	24.2	7.0	A
		99O008D	11	250-580	0.70	0.89	12.26	27.7 ± 1.4	26.3	7.6	A
		99O008E	13	150-580	0.80	0.91	27.02	21.2 ± 0.6	20.7	6.0	A
		99O008F	12	200-580	0.73	0.90	16.67	22.0 ± 0.9	20.9	6.1	A
Mean[1]								24.7	**23.5**	**6.8**	
***σ*[1]**								2.7	**2.3**	**0.7**	
OAX09 (B.R.H.)	San José (1150–850 BC)	99O009A	Arai diagrams are very flat, Zijderveld projections are very scattered and do not point to the origin, pTRM checks failed.								D
		99O009B									D
		99O009C									D
		99O009D									D
		99O009E									D
		99O009F									D
OAX10 (S.J.M.)	San José (1150–850 BC)	99O010B	9	150-500	0.53	0.86	16.59	25.6 ± 0.7	25.3	7.3	B
		99O010C	7	200-475	0.49	0.82	14.15	33.5 ± 0.9	31.7	9.2	B
		99O010E	5	350-500	0.41	0.74	7.55	23.9 ± 1.0	22.9	6.7	B
		99O010F	6	350-520	0.50	0.79	12.29	18.6 ± 0.6	17.7	5.1	B
Mean[1]								26.8	**25.8**	**7.5**	
***σ*[1]**								6.2	**5.7**	**1.7**	
OAX11	San José	99O011A	7	450-580	0.47	0.83	7.35	35.9 ± 1.9	34.3	10.0	A

(Origin?)	(1150–850 BC)	99O011B	7	450-580	0.45	0.82	16.26	39.6 ± 0.9	38.0	11.0	A
		99O011C	6	475-580	0.43	0.79	16.21	37.8 ± 0.8	36.7	10.7	A
		99O011D	7	450-580	0.47	0.83	17.37	34.9 ± 0.8	33.6	9.7	A
		99O011E	Broken at 500°C.								
		99O011F	7	450-580	0.47	0.82	12.00	32.2 ± 1.0	31.0	9.0	A
Mean[1]								35.4	**34.1**	**9.9**	
σ[1]								2.9	**2.8**	**0.8**	
OAX12 (S.J.M.)	San José (1150–850 BC)	99O012A	7	400-560	0.59	0.82	7.37	32.3 ± 2.1	30.6	8.9	C[2]
		99O012B	8	350-560	0.70	0.84	18.24	35.5 ± 1.1	34.3	9.9	C[2]
		99O012C	Arai diagram is concave-up whereas Zijderveld diagram is linear.								C
		99O012D	Arai diagram is concave-up whereas Zijderveld diagram is linear.								C
		99O012E	Broken at 540°C.								
		99O012F	Arai diagram is concave-up whereas Zijderveld diagram is linear.								C
OAX13 (S.J.M.)	Tierras Largas (1400–1150 BC)	99O013A	8	400-580	0.82	0.83	17.59	38.1 ± 1.5	37.8	11.0	A
		99O013B	8	400-580	0.83	0.82	14.74	36.2 ± 1.7	35.8	10.4	A
		99O013C	8	350-560	0.81	0.82	15.58	39.9 ± 1.7	39.7	11.5	A
		99O013D	9	350-580	0.81	0.83	16.09	39.9 ± 1.7	39.3	11.4	A
		99O013E	8	400-580	0.77	0.82	15.67	31.9 ± 1.3	31.6	9.2	A
		99O013F	Broken at 580°C before cooling rate measurements.								
Mean[1]								36.3	**35.9**	**10.4**	
σ[1]								4.1	**4.0**	**1.2**	
OAX14 (S.J.M.)	San José (1150–850 BC)	99O014B	Arai diagrams and Zijderveld projections are very scattered as for potsherd OAX09. Specimens do not demagnetize even after heating to 580°C and pTRM checks failed.								D
		99O014C									D
		99O014D									D
		99O014E									D
		99O014F									D
OAX15 (S.J.M.)	San José (1150–850 BC)	99O015A	Arai and Zijderveld diagrams are scattered, pTRM checks fail, alteration factor is bigger than 15% for specimens 99O015B and 99O015C.								D
		99O015B									D
		99O015C									D
		99O015D									D

		99O015E									D
		99O015F									D
OAX16 (S.J.M.)	Tierras Largas (1400–1150 BC)	99O016A	9	350-580	0.79	0.86	17.04	24.4 ± 1.0	22.8	6.6	A
		99O016B	Broken at 475°C.								
		99O016C	9	300-560	0.57	0.86	20.41	29.2 ± 0.7	27.6	8.0	A
		99O016D	Broken at 400°C.								
		99O016E	11	250-580	0.69	0.87	23.94	23.8 ± 0.6	22.6	6.6	A
		99O016F	11	200-560	0.59	0.88	10.94	26.3 ± 1.3	25.1	7.3	A
Mean[1]								26.2	**24.7**	**7.2**	
***σ*[1]**								2.6	**2.5**	**0.7**	
OAX17 (S.J.M.)	Tierras Largas (1400–1150 BC)	99O017A	Broken at 400°C.								
		99O017B	11	250-580	0.77	0.89	20.44	31.0 ± 1.0	29.6	8.6	A
		99O017C	Broken at 350°C.								
		99O017D	8	400-580	0.60	0.85	19.28	34.8 ± 0.9	32.6	9.4	A
		99O017E	Broken at 350°C.								
		99O017F	10	250-560	0.73	0.84	22.89	23.1 ± 0.6	22.0	6.4	A
Mean[1]								29.6	**28.0**	**8.1**	
***σ*[1]**								6.0	**5.5**	**1.6**	

[1]The values in bold and underlined in gray, corrected for both cooling rate and anistotropy effect (see "Cooling-rate correction" and "Anisotropy correction" sections for detailed explanations), are those that were used for final F_{cor} and VADM mean calculation for each Formative phase.

[2]Specimens 99O012A and 99O012B have a very small concave-up shape but a sufficiently linear Arai diagrams to consider that the calculation of a reliable paleointensity is possible.

Supplemental material 2: Archeointensity results for the 15 studied potsherds from the Oaxaca Valley. From left to right: name of the potsherd and corresponding site of origin (S.J.M. = San José Mogote, T.L. = Tierras Largas, B.R.H. = Barrio del Rosario Huitzo); phase in the Formative period and associated ages; studied specimens per potsherd; *N* is the number of heating steps used for archeointensity estimate; ΔT (°C) is the temperature interval used for archeointensity determination; *f* is the NRM fraction; *g* is the gap factor; *q* is the quality factor defined by Coe *et al.* (1978); $F \pm \sigma F$ (μT) is the raw archeointensity value and its standard deviation, before any correction; F_{cor} (μT) is the archeointensity value after cooling rate corrections; VADM is the Virtual Axial Dipole Moment calculated for the location of Oaxaca (latitude: 17.07°N; longitude: 96.72°W). Underlined in gray (in white) are indicated specimens that are reliable (that fail).